ROBUST REMOVAL OF FIXED PATTERN NOISE ON MULTI-FOCUS IMAGES

Kazuya Kodama[⋆] *Kenta Fukui*[⋆,†] *Takayuki Hamamoto*[†]

[⋆] National Institute of Informatics, Research Organization of Information and Systems
2–1–2 Hitotsubashi, Chiyoda-ku, Tokyo 101–8430, Japan
[†] Graduate School of Engineering, Tokyo University of Science
6–3–1 Niijuku, Katsushika-ku, Tokyo 125–8585, Japan

ABSTRACT

In this paper, we propose a novel method restoring multi-focus images based on convex optimization with new constraint for fixed pattern noise. Even weak fixed pattern noise on multi-focus images degrades all-in-focus images reconstructed by linear combination of them, especially, when using telecentric optical systems such as microscopes. Our novel method introduces constraint for additive fixed pattern noise into total variation minimization and then it is improved for multiplicative fixed pattern noise. The proposed method suppresses fixed pattern noise on multi-focus images very robustly to avoid such degradation on reconstructed images. Experimental results show that our method achieves high performance compared to simple total variation minimization.

Index Terms— focus, image reconstruction, fixed pattern noise, image restoration, convex optimization

1. INTRODUCTION

Our previously proposed image reconstruction from multi-focus images for efficient scene refocusing without any depth estimation adopts linear combination of them in the frequency domain [1]. However, our image reconstruction suffers from severe degradation only if using telecentric optical systems such as microscopes and reconstructing simple all-in-focus images. Even weak fixed pattern noise on multi-focus images acquired by microscopes is directly integrated by our linear filters in the frequency domain into such artifacts on reconstructed all-in-focus images because each filter works as a high-pass filter to extract regions in focus from the multi-focus images. In order to obtain better quality of all-in-focus images, we need to suppress fixed pattern noise on multi-focus images very robustly before image reconstruction.

Many researchers adopted total variation minimization [2, 3, 4] as effective optimization for image denoising and it has been greatly improved for various applications in recent years [5, 6, 7]. On the other hand, non-local image denoising integrating similar regions found by block matching is also known to be very effective [8, 9]. Actually, it is extended to video denoising [10, 11] and multi-view image denoising [12, 13], and they show significant performance for strong noise. However, noise on multiple images is not directly analyzed well based on integration of them to deal with even weak noise robustly. In this paper, we propose a novel method for restoration of multi-focus images, that is unique and hardly investigated in comparison with video denoising [14], based on convex optimization by introducing new constraint on solution sets for fixed pattern noise into total variation minimization. On blurred regions of multi-focus images, weak fixed pattern noise can be detected and precisely suppressed, and those regions are expected to help clear textures to be well preserved without over-smoothing.

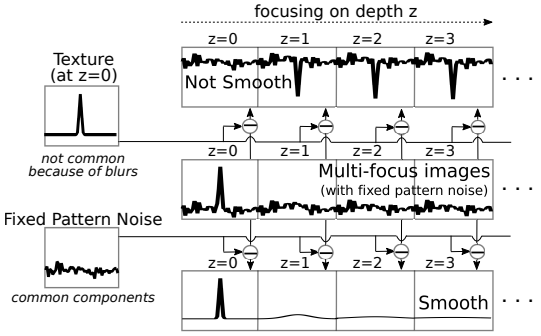

Fig. 1. Smoothness of multi-focus images increases only if their common components (fixed pattern noise) are removed.

We show experimental results using synthetic and real images with additive or multiplicative fixed pattern noise. Our proposed method is evaluated and compared with conventional image denoising by reconstructing all-in-focus images after restoration of multi-focus images.

2. RESTORATION OF MULTI-FOCUS IMAGES

2.1. Removal of Additive Fixed Pattern Noise

Because multi-focus images mainly consist of smoothly blurred regions, effective image denoising is easily achieved except for regions in focus by optimization minimizing an

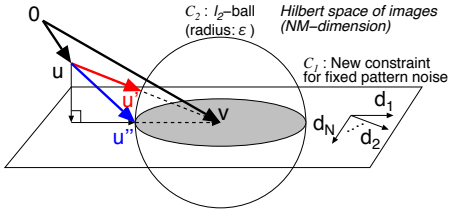

Fig. 2. Modification of convex projection for new constraint on solution sets.

appropriate objective function such as total variation. In addition, in the case of fixed pattern noise, we may introduce constraint on solution sets into such optimization, where pixel values at the same position on multi-focus images are to be equally increased or decreased.

Actually, as shown in Fig.1, if incorrectly suppressing textures in focus, variations of blurred regions greatly increase. On the other hand, if correctly suppressing fixed pattern noise, variations of them successfully decrease. As a result, our approach is expected to only suppress fixed pattern noise precisely in avoiding over-smoothing.

In this paper, under the above-mentioned constraint, restoration of multi-focus images with additive fixed pattern noise [15] is formulated as a convex optimization problem to minimize the variations of them in Eq.(1).

$$\begin{aligned} &\hat{\mathbf{u}} = \arg\min_{\mathbf{u}} J(\mathbf{u}) + F_{\mathbf{v}}(\mathbf{u}) \\ &s.t.\ \forall (i,j) \in W \times H,\ \left(\mathbf{u}_{(i,j)} - \mathbf{v}_{(i,j)}\right) \parallel \mathbf{d}, \end{aligned} \tag{1}$$

where multi-focus images $\mathbf{g}_k \in \mathbb{R}^N\,(k = 1, ..., M)$, having $N\,(= N_h \times N_v)$ pixels, are merged into a single image, $\mathbf{v} = \left(\mathbf{g}_1^\top ... \mathbf{g}_M^\top\right)^\top \in \mathbb{R}^{NM}$. Here, we evaluate smoothness of an image by using total (generalized) variation as $J \in \{J_{TV}, J_{TGV}^{\alpha}\}$ [5, 6]. $F_{\mathbf{v}}$ is an indicator function of ℓ_2 norm ball $\mathcal{B}^2_{\mathbf{v},\varepsilon} := \{\mathbf{u} \in \mathbb{R}^{NM} \mid \|\mathbf{u} - \mathbf{v}\|_2 \leq \varepsilon\}$. That is to say, $F_{\mathbf{v}}(\mathbf{u})$ is 0 if $\mathbf{u}$ is inside of the ball, and it is $+\infty$ if $\mathbf{u}$ is outside of the ball.

We determine ε by using standard deviation σ of the fixed pattern noise, that is given or can be estimated. For example, $\varepsilon = \sqrt{NM}\sigma$ is simple and appropriate. In the constraint of Eq.(1), $W \times H = \{1, ..., N_h\} \times \{1, ..., N_v\}$ represents all the pixel positions on the image sensor and $\mathbf{v}_{(i,j)}, \mathbf{u}_{(i,j)} \in \mathbb{R}^M$ represent vectors which are composed of M pixel values corresponding to the same position (i, j) on the original multi-focus images $\mathbf{g}_k\,(k = 1, ..., M)$ and restored ones, respectively. Then, this constraint keeps difference between the vectors parallel to $\mathbf{d} = (1, ..., 1) \in \mathbb{R}^M$ and pixel values at the same position on multi-focus images are equally increased or decreased after image restoration. Such restoration results in suppressing only fixed pattern noise very robustly.

Fig.2 shows the constraint on solution sets for fixed pattern noise. We define subset C_1 for new constraint using the vector space spanned by $S = \{\mathbf{d}_k \in \mathbb{R}^{NM} \mid k = 1, .., N\}$, where only M elements corresponding to the k-th pixel on the image sensor are set to 1 on $\mathbf{d}_k$, while the other elements are set to 0. Subset C_1 including $\mathbf{v}$ is parallel to the vector space. Subset C_2 is ordinary constraint of ℓ_2 norm ball around $\mathbf{v}$. Finally, the constraint for fixed pattern noise becomes $\mathbf{u} \in C_1 \cap C_2$, that is a gray region in Fig.2.

Algorithm 1: Solver for (2) with $J = J_{TGV}^{\alpha}$

input : $\mathbf{u}^{(0)}, \mathbf{p}^{(0)}, \mathbf{z}^{(0)} := [\mathbf{z}_1^{(0)}, \mathbf{z}_2^{(0)}]$
output: $\mathbf{u}^{(n)}$
while *A stopping criterion is not satisfied* **do**
- $\mathbf{u}^{(n+1)} = \mathrm{prox}_{\gamma_1 \hat{F}_{\mathbf{v}}}\left(\mathbf{u}^{(n)} - \gamma_1\left(\mathbf{D}_1^\top \mathbf{z}_1^{(n)}\right)\right)$;
- $\mathbf{p}^{(n+1)} = \mathbf{p}^{(n)} - \gamma_1\left(-\mathbf{z}_1^{(n)} + \mathbf{G}_1^\top \mathbf{z}_2^{(n)}\right)$;
- $\mathbf{t}_1^{(n)} = \mathbf{z}_1^{(n)} + \gamma_2\left(\mathbf{D}_1\left(2\mathbf{u}^{(n+1)} - \mathbf{u}^{(n)}\right) - \left(2\mathbf{p}^{(n+1)} - \mathbf{p}^{(n)}\right)\right)$;
- $\mathbf{t}_2^{(n)} = \mathbf{z}_2^{(n)} + \gamma_2\left(\mathbf{G}_1\left(2\mathbf{p}^{(n+1)} - \mathbf{p}^{(n)}\right)\right)$;
- $\mathbf{z}_1^{(n+1)} = \mathbf{t}_1^{(n)} - \gamma_2 \mathrm{prox}_{\frac{\alpha}{\gamma_2}\|\cdot\|_{1,2}}\left(\frac{1}{\gamma_2}\mathbf{t}_1^{(n)}\right)$;
- $\mathbf{z}_2^{(n+1)} = \mathbf{t}_2^{(n)} - \gamma_2 \mathrm{prox}_{\frac{(1-\alpha)}{\gamma_2}\|\cdot\|_{1,2}}\left(\frac{1}{\gamma_2}\mathbf{t}_2^{(n)}\right)$;
- $n \longleftarrow n + 1$;

Here, we combine the new constraint and the objective function using $F_{\mathbf{v}}$ in Eq.(1) into the following one using $\hat{F}_{\mathbf{v}}$ in Eq.(2), where $\hat{F}_{\mathbf{v}}(\mathbf{u})$ is 0 in $C_1 \cap C_2$ and it gets $+\infty$ outside of it.

$$\hat{\mathbf{u}} = \arg\min_{\mathbf{u}} J(\mathbf{u}) + \hat{F}_{\mathbf{v}}(\mathbf{u}) \tag{2}$$

Algorithm 1 is an iterative procedure to solve Eq.(2) of $J = J_{TGV}^{\alpha}$, that is obtained by applying a primal-dual splitting (PDS) method [16, 17] to the equation. Specifically, we refer to the paper for color image denoising [6] and its procedure is modified as follows: J and $\hat{F}_{\mathbf{v}}$ are assigned to different convex functions for PDS and color, deblurring and dynamic range of $\mathbf{u} \in [0, 255]^{NM}$ are excluded from consideration.

In addition, as shown in Fig.2, $\mathrm{prox}_{\gamma F_{\mathbf{v}}}$ [6] for obtaining $\mathbf{u}'$ by convex projection of $\mathbf{u}$ on ℓ_2 norm ball is replaced with $\mathrm{prox}_{\gamma \hat{F}_{\mathbf{v}}}$ for obtaining $\mathbf{u}''$ by convex projection of $\mathbf{u}$ on the subset $C_1 \cap C_2$ corresponding to fixed pattern noise. We implement $\mathrm{prox}_{\gamma \hat{F}_{\mathbf{v}}}$ with the first convex projection on C_1 and the second convex projection on ℓ_2 norm ball to obtain $\mathbf{u}''$.

2.2. Removal of Multiplicative Fixed Pattern Noise

Degradation by multiplicative noise can be formulated as $v = u\eta$, where u and v are pixel values before and after degradation, respectively, and η has a distribution of mean 1 and variance ${\sigma_m}^2$ [3, 18]. Multiplicative fixed pattern noise varying spatially on image sensors is caused by PRNU (photo response non-uniformity) that has an approximately normal distribution [19]. Therefore, we adopt simple $v = u(1 + w)$, where w has a normal distribution $N\left(0, {\sigma_m}^2\right)$.

In this paper, we apply logarithmic transformation to pixel values in order to convert multiplicative fixed pattern noise to additive components as follows: $\log(v) = \log(u) + \log(1 + w)$.

Table 1. n-th order approximation of μ_t and ${\sigma_{mt}}^2$.

n	μ_t	${\sigma_{mt}}^2$
1	0	${\sigma_m}^2$
2	$-\frac{1}{2}{\sigma_m}^2$	${\sigma_m}^2+\frac{1}{2}{\sigma_m}^4$
3	$-\frac{1}{2}{\sigma_m}^2$	${\sigma_m}^2+\frac{5}{2}{\sigma_m}^4+\frac{5}{3}{\sigma_m}^6$
4	$-\frac{1}{2}{\sigma_m}^2-\frac{3}{4}{\sigma_m}^4$	${\sigma_m}^2+\frac{5}{2}{\sigma_m}^4+\frac{14}{3}{\sigma_m}^6+6{\sigma_m}^8$
5	$-\frac{1}{2}{\sigma_m}^2-\frac{3}{4}{\sigma_m}^4$	${\sigma_m}^2+\frac{5}{2}{\sigma_m}^4+\frac{32}{3}{\sigma_m}^6+20{\sigma_m}^8+\frac{189}{5}{\sigma_m}^{10}$

Then, the proposed method in the previous subsection can be easily improved for multiplicative fixed pattern noise. We note that mean μ_t and variance ${\sigma_{mt}}^2$ of fixed pattern noise after logarithmic transformation are not equal to 0 and ${\sigma_m}^2$, respectively. Actually, because $\log(1+w) = \sum_{n=1}^{\infty}\frac{(-1)^{n-1}}{n}w^n \ (|w|<1)$ and

$$\mathrm{E}[w^n] = \begin{cases} 0 & (\text{if } n \text{ is odd}) \\ {\sigma_m}^n\,(n-1)\cdot(n-3)\cdot\ldots\cdot 3\cdot 1 & (\text{if } n \text{ is even}) \end{cases},$$

we can obtain approximation of μ_t and ${\sigma_{mt}}^2$ as shown in Tab.1.

Here, we simply replace logarithmic transformation $\log(v)$ with $\log(v)-\mu_t$. Then, the center of the ℓ_2 norm ball only shifts and remains on new constraint C_1 for fixed pattern noise because μ_t is constant. We set the radius to $\varepsilon = \sqrt{NM}\sigma_{mt}$. Finally, we can apply Algorithm 1 to multi-focus images with multiplicative fixed pattern noise after the transformation. Of course, in order to obtain restored multi-focus images from optimized $\hat{\mathbf{u}}$ by Algorithm 1, we need to apply inverse transformation to each element u of $\hat{\mathbf{u}}$ by using the ordinary exponential function e^u.

3. EXPERIMENTS

3.1. Simulations for Additive Fixed Pattern Noise

For simulations in this section, we prepare multi-focus images $\mathbf{x}_k\ (k=1,...,64)$ as ground truth by placing "Barbara"(128×128 pixels) orthogonal to the depth direction at $k=33$. There are Gaussian blurs on $\mathbf{x}_k$ by setting $r=1.0$ as our 3D blurring parameter corresponding to the radius of the iris [1, 20, 21]. Then, we add fixed pattern noise of normal distribution $N\left(0,{\sigma_a}^2\right)$ and random noise of $N\left(0,{\sigma_{ra}}^2\right)$ to $\mathbf{x}_k$, where noisy multi-focus images $\mathbf{g}_k$ are obtained after 8 bit quantization for our simulations. We note that random noise on $\mathbf{g}_k$ is independent of that on $\mathbf{g}_{k'}$ if $k\neq k'$, while fixed pattern noise on $\mathbf{g}_k$ is identical to that on $\mathbf{g}_{k'}$. We control the radius of ℓ_2 norm ball in consideration of the noise level by $\varepsilon=\sqrt{NM}\sigma_a\ (N=128\times 128, M=64)$ and we always set $\alpha=0.5, \gamma_1=0.01, \gamma_2=1/(12\gamma_1)$ in Algorithm 1. In addition, we adopt $\|\mathbf{u}^{(n+1)}-\mathbf{u}^{(n)}\|_2/\|\mathbf{u}^{(n)}\|_2 \leq 10^{-6}$ as a stopping criterion.

At first, in Fig.3(a), multi-focus images and reconstructed all-in-focus images with or without the proposed image restoration are shown, where $\sigma_a = 0, 1, 10$ from left to right. Fig.3(c) indicates quality of them when varying σ_a. At $\sigma_a = 0.5$, quality of the reconstructed all-in-focus image significantly increases from 20.6[dB] to 38.3[dB] after restoration of multi-focus images. Even at $\sigma_a = 10$, it keeps good quality of 34.3[dB]. Note that we calculate the PSNR in Fig.3(c) after 8 bit quantization, except for restored multi-focus images, that are treated by floating point numbers, and random noise does not exist ($\sigma_{ra}=0$) in this simulation. For comparison, in Fig.3(b), we show reconstructed all-in-focus images after restoration of multi-focus images by using simple TGV instead of our method, where $\hat{F}_{\mathbf{v}}$ is replaced with the original $F_{\mathbf{v}}$ of Eq.(1) in Algorithm 1. In Fig.3(c), quality of them is also shown. As we see in Fig.3(b), larger σ_a degrades reconstructed all-in-focus images with visible artifacts.

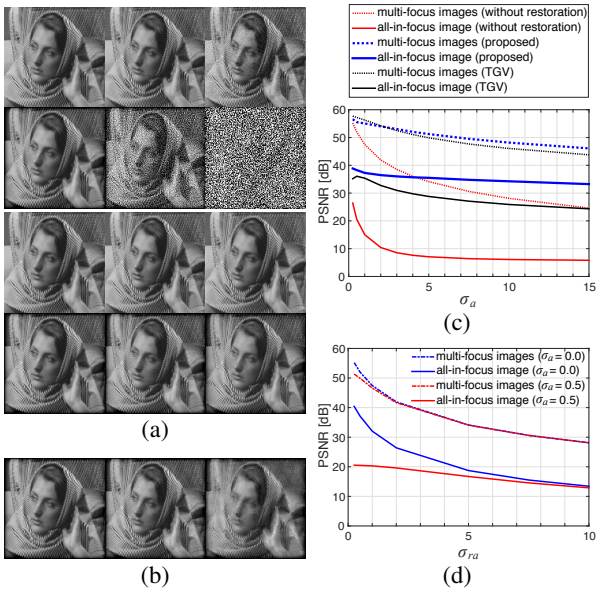

Fig. 3. Effects of additive fixed pattern noise on multi-focus images and reconstructed images: (a) images in focus and reconstructed images without restoration (upper 6 images) and those after restoration (lower); from left to right, $\sigma_a=0, 1, 10$, (b) reconstructed images after restoration using simple TGV, (c) performance comparison, (d) effects of random noise.

Next, in order to evaluate effects of fixed pattern noise compared to those of random noise, quality of multi-focus images and reconstructed all-in-focus images without any restoration is analyzed by varying σ_{ra} in Fig.3(d). When only random noise exists ($\sigma_a = 0$), quality of reconstructed all-in-focus images decreases to 18.7[dB] at $\sigma_{ra}=5$. However, when even weak fixed pattern noise exists ($\sigma_a = 0.5$), it cannot go over 20.6[dB] regardless of random noise. We notice that it is important for all-in-focus image reconstruction by linear combination of multi-focus images to suppress even weak fixed pattern noise robustly rather than random noise.

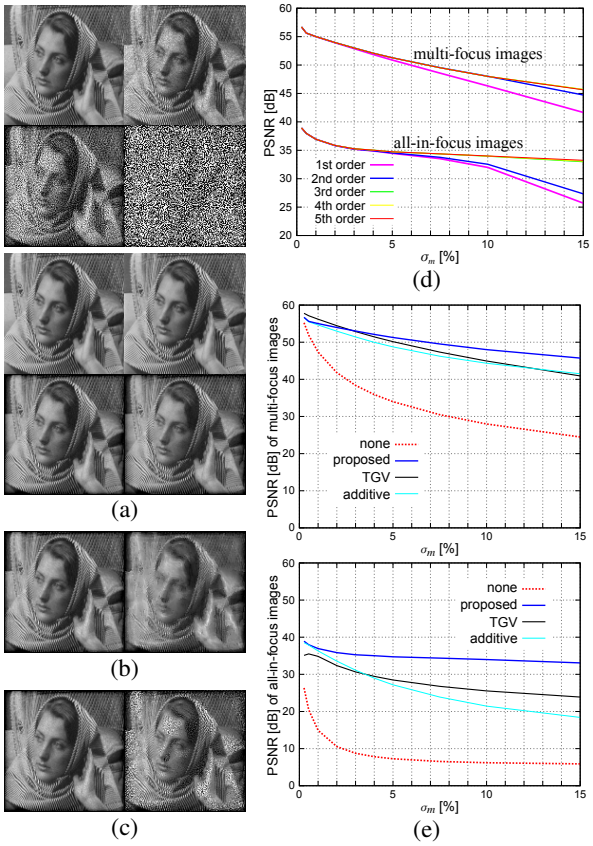

Fig. 4. Effects of multiplicative fixed pattern noise on multi-focus images and reconstructed images: (a) images in focus and reconstructed images without restoration (upper 2×2) and those after restoration (lower) at $\sigma_m[\%] = 1$ (left), 10 (right), (b) reconstructed images after restoration using simple TGV, (c) reconstructed images after restoration for additive noise, (d) precision of approximation, (e) performance comparison.

3.2. Simulations for Multiplicative Fixed Pattern Noise

In this subsection, multi-focus images $\mathbf{g}_k$ are prepared by adding multiplicative fixed pattern noise of $N\left(0, {\sigma_m}^2\right)$ to $\mathbf{x}_k$. We achieve restoration through the proposed transformation and its inverse in Sec.2.2. Except for ε, all the other parameters are set in the same way as the previous simulations. Then, experimental results in Fig.4(a) are obtained, where ε is determined as described in Sec.2.2 with 4-th order approximation in Tab.1. According to Fig.4(d) indicating quality of multi-focus images and reconstructed all-in-focus images after restoration with n-th order approximation, we adopt $n=4$.

For comparison, in Fig.4(b) and Fig.4(c), we also show reconstructed all-in-focus images after restoration of multi-focus images by using simple TGV and by directly using the proposed method for additive noise in Sec.2.1, respectively. The latter uses $\varepsilon = \sqrt{NM}\sigma_m \bar{\mathrm{v}}$ ($\bar{\mathrm{v}}$: the average pixel value of $\mathbf{v}$). Our proposed method for multiplicative noise is superior to the other methods, as we also see in Fig.4(e), where quality of those images is indicated by varying σ_m. We notice that, at $\sigma_m = 10\%$, severe degradation exists on bright regions in Fig.4(c), where the noise gets much stronger than that of $\sigma_m \bar{\mathrm{v}}$.

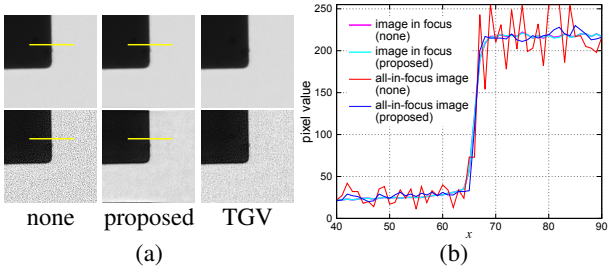

Fig. 5. Experimental results using real images: images in focus and reconstructed all-in-focus images; (a) from left to right, no restoration, our proposed restoration and restoration using simple TGV, (b) pixel values on the line in (a).

3.3. Experiments Using Real Images

In this subsection, we use real multi-focus images ($N = 128 \times 128, M = 64$), that are acquired by Olympus BX61 microscope with ORCA-Flash2.8. Our 3D blurring parameter $r = 1.25$ and standard deviation $\sigma_m = 0.5\%$ of multiplicative fixed pattern noise caused by the image sensor are estimated in advance [20, 21, 22]. In Fig.5(a), we show multi-focus images and reconstructed all-in-focus images with or without restoration. Fig.5(b) indicates pixel values on the line of those images shown in Fig.5(a). We see good quality of the reconstructed all-in-focus image after our proposed restoration. For comparison, we also show those after restoration using simple TGV in Fig.5(a), where the reconstructed image is degraded severely in comparison with the previous simulations. Such simple TV-based methods tend to suppress dominant random noise in real images rather than weak fixed pattern noise causing the degradation. Experimental results show robustness of our proposed method for removal of fixed pattern noise.

4. CONCLUSIONS AND FUTURE WORKS

We proposed a novel method for removing fixed pattern noise on multi-focus images accurately by achieving such restoration as convex optimization with new constraint for the noise. Experimental results show robustness of our proposed method for all-in-focus image reconstruction using linear combination of multi-focus images with additive or multiplicative fixed pattern noise even in the case of real images.

In the future, we will extend our method to remove more complex noise including both additive and multiplicative components. For further quality improvement, suppression of dominant random noise on real images needs to be integrated.

5. REFERENCES

[1] Kazuya Kodama and Akira Kubota, "Efficient reconstruction of all-in-focus images through shifted pinholes from multi-focus images for dense light field synthesis and rendering," *IEEE Trans. Image Processing*, vol. 22, no. 11, pp. 4407–4421, 2013.

[2] Leonid I Rudin, Stanley Osher, and Emad Fatemi, "Nonlinear total variation based noise removal algorithms," *Physica D: Nonlinear Phenomena*, vol. 60, no. 1, pp. 259–268, 1992.

[3] Leonid I. Rudin and Stanley Osher, "Total variation based image restoration with free local constraints," in *Proc. IEEE International Conference on Image Processing*, Nov. 1994, vol. 1, pp. 31–35.

[4] Antonin Chambolle, "An algorithm for total variation minimization and applications," *J. Mathematical Imaging and Vision*, vol. 20, no. 1–2, pp. 89–97, 2004.

[5] Kristian Bredies, Karl Kunisch, and Thomas Pock, "Total generalized variation," *SIAM J. Imaging Sciences*, vol. 3, no. 3, pp. 492–526, 2010.

[6] Shunsuke Ono and Isao Yamada, "Decorrelated vectorial total variation," in *Proc. IEEE Conference on Computer Vision and Pattern Recognition*, June 2014, pp. 4090–4097.

[7] Xi-Le Zhao, Fan Wang, and Michael K. Ng, "A new convex optimization model for multiplicative noise and blur removal," *SIAM J. Imaging Sciences*, vol. 7, no. 1, pp. 456–475, 2014.

[8] Antoni Buades, Bartomeu Coll, and Jean-Michel Morel, "A non-local algorithm for image denoising," in *Proc. IEEE Conference on Computer Vision and Pattern Recognition*, June 2005, vol. 2, pp. 60–65.

[9] Kostadin Dabov, Alessandro Foi, Vladimir Katkovnik, and Karen Egiazarian, "Image denoising by sparse 3-d transform-domain collaborative filtering," *IEEE Trans. Image Processing*, vol. 16, no. 8, pp. 2080–2095, 2007.

[10] Kostadin Dabov, Alessandro Foi, and Karen Egiazarian, "Video denoising by sparse 3d transform-domain collaborative filtering," in *Proc. European Signal Processing Conference*, Sept. 2007, pp. 145–149.

[11] Matteo Maggioni, Giacomo Boracchi, Alessandro Foi, and Karen Egiazarian, "Video denoising, deblocking, and enhancement through separable 4-d nonlocal spatiotemporal transforms," *IEEE Trans. Image Processing*, vol. 21, no. 9, pp. 3952–3966, 2012.

[12] Li Zhang, Sundeep Vaddadi, Hailin Jin, and Shree K Nayar, "Multiple view image denoising," in *Proc. IEEE Conference on Computer Vision and Pattern Recognition*, June 2009, pp. 1542–1549.

[13] Enming Luo, Stanley H. Chan, Shengjun Pan, and Truong Q Nguyen, "Adaptive non-local means for multiview image denoising: Searching for the right patches via a statistical approach," in *Proc. IEEE International Conference on Image Processing*, Sept. 2013, pp. 543–547.

[14] Matteo Maggioni, Enrique Sanchez-Monge, and Alessandro Foi, "Joint removal of random and fixed-pattern noise through spatiotemporal video filtering," *IEEE Trans. Image Processing*, vol. 23, no. 10, pp. 4282–4296, 2014.

[15] Tomochika Murakami, Masanori Sato, Zhen Wang, and Kazuya Kodama, "Signal recovery for multi-focus images with fixed pattern noise," *IEICE Trans. Information and Systems*, vol. J99-D, no. 8, pp. 809–812, 2016.

[16] Antonin Chambolle and Thomas Pock, "A first-order primal-dual algorithm for convex problems with applications to imaging," *J. Mathematical Imaging and Vision*, vol. 40, no. 1, pp. 120–145, 2011.

[17] Laurent Condat, "A primal-dual splitting method for convex optimization involving lipschitzian, proximable and linear composite terms," *J. Optimization Theory and Applications*, vol. 158, no. 2, pp. 460–479, 2013.

[18] Gilles Aubert and Jean-Francois Aujol, "A variational approach to removing multiplicative noise," *SIAM J. Applied Mathematics*, vol. 68, no. 4, pp. 925–946, 2008.

[19] Mikhail Konnik and James Welsh, "High-level numerical simulations of noise in ccd and cmos photosensors: review and tutorial," *arXiv preprint arXiv:1412.4031v1 [astro-ph.IM]*, Dec. 2014.

[20] Kazuya Kodama, Hiroshi Mo, and Akira Kubota, "Free iris scene re-focusing based on a three-dimensional filtering of multiple differently focused images," in *Proc. IEEE International Conference on Image Processing*, Oct. 2006, pp. 2033–2036.

[21] Kazuya Kodama, Hiroshi Mo, and Akira Kubota, "Simple and fast all-in-focus image reconstruction based on three-dimensional/two-dimensional transform and filtering," in *Proc. IEEE International Conference on Acoustics, Speech and Signal Processing*, Apr. 2007, vol. 1, pp. 769–772.

[22] European Machine Vision Association, *EMVA Standard 1288: Standard for Characterization of Image Sensors and Cameras, Release 3.0, Nov. 29, 2010*.